



Cra and cAMP Receptor Protein Have Opposing Roles in the Regulation of *fruB* in *Vibrio cholerae*

Christina Beck,^{a*} Sayde Perry,^a Daniel M. Stoebel,^b Jane M. Liu^a

^aDepartment of Chemistry, Pomona College, Claremont, California, USA

^bDepartment of Biology, Harvey Mudd College, Claremont, California, USA

ABSTRACT The Gram-negative bacterium *Vibrio cholerae* adapts to changes in the environment by selectively producing the necessary machinery to take up and metabolize available carbohydrates. The import of fructose by the fructose-specific phosphoenolpyruvate (PEP) phosphotransferase system (PTS) is of particular interest because of its putative connection to cholera pathogenesis and persistence. Here, we describe the expression and regulation of *fruB*, which encodes an EIIA-FPr fusion protein as part of the fructose-specific PTS in *V. cholerae*. Using a series of transcriptional reporter fusions and additional biochemical and genetic assays, we identified Cra (catabolite repressor/activator) and cAMP receptor protein (CRP) as regulators of *fruB* expression and determined that this regulation is dependent upon the presence or absence of PTS sugars. Cra functions as a repressor, downregulating *fruB* expression in the absence of fructose when components of PTS^{Fru} are not needed. CRP functions as an activator of *fruB* expression. We also report that Cra and CRP can affect *fruB* expression independently; however, CRP can modulate *cra* expression in the presence of fructose and glucose. Evidence from this work provides the foundation for continued investigations into PTS^{Fru} and its relationship to the *V. cholerae* life cycle.

IMPORTANCE *Vibrio cholerae* is the causative agent of cholera disease. While current treatments of care are accessible, we still lack an understanding of the molecular mechanisms that allow *V. cholerae* to survive in both aquatic reservoirs and the human small intestine, where pathogenesis occurs. Central to *V. cholerae*'s survival is its ability to use available carbon sources. Here, we investigate the regulation of *fruB*, which encodes a protein central to the import and metabolism of fructose. We show that *fruB* expression is controlled by the transcriptional regulators Cra and CRP. This work contributes toward a clearer understanding of how carbon source availability impacts the physiology and, potentially, the persistence of the pathogen.

KEYWORDS CRP, Cra, FPr, FruR, PTS, *Vibrio cholerae*, fructose

Caused by the facultative pathogen *Vibrio cholerae*, cholera disease is estimated to affect three to five million people each year and is characterized by profuse, watery diarrhea, resultant dehydration, and hypovolemic shock (1, 2). While current intravenous and oral rehydration treatments are effective in treating the disease, approximately 1.3 billion people across 51 countries are still at risk for infection due to gaps in health infrastructure (1, 3, 4). The transmission of *V. cholerae* is most frequently attributed to malfunctioning or inadequate sanitation systems, as well as the lack of clean water sources (1, 3). Important to this transmission is the ability of *V. cholerae* to adapt to conditions in both the human small intestine, where pathogenesis occurs, and aquatic reservoirs, where the bacteria spread between contaminated water sources (5, 6). In order to survive in both niches, *V. cholerae* must sense the carbon sources currently available and produce the necessary metabolic machinery to convert available

Citation Beck C, Perry S, Stoebel DM, Liu JM. 2021. Cra and cAMP receptor protein have opposing roles in the regulation of *fruB* in *Vibrio cholerae*. *J Bacteriol* 203:e00044-21. <https://doi.org/10.1128/JB.00044-21>.

Editor Conrad W. Mullineaux, Queen Mary University of London

Copyright © 2021 Beck et al. This is an open-access article distributed under the terms of the [Creative Commons Attribution 4.0 International license](https://creativecommons.org/licenses/by/4.0/).

Address correspondence to Jane M. Liu, jane.liu@pomona.edu.

* Present address: Christina Beck, Department of Biology, Massachusetts Institute of Technology, Cambridge, Massachusetts, USA.

Received 25 January 2021

Accepted 23 February 2021

Accepted manuscript posted online

1 March 2021

Published 21 April 2021

carbon sources to utilizable energy currency (7). The phosphoenolpyruvate (PEP) phosphotransferase system (PTS), a phosphotransfer cascade conserved across many bacterial species and responsible for carbon uptake and phosphorylation for downstream metabolism, is thought to play a role in *V. cholerae*'s ability to survive in multiple environments (7).

The PTS phosphocascade begins with the transfer of a phosphate group from PEP to EI, a constitutively expressed cytoplasmic protein (8, 9). Next, the phosphate group is passed from EI to histidine protein (HPr or the HPr homolog FPr), another cytoplasmic component (8, 9). From HPr or FPr, the phosphate group is then passed to a number of carbohydrate-specific domains, referred to as EIIC and EIIB (8, 9). Intake of the carbohydrate across the membrane then occurs via the EIIC domain, a carbohydrate-specific transmembrane protein (8, 9). The carbohydrate is concomitantly phosphorylated with this transport step (8, 9). Because carbon specificity lies within the domains of the EIIC protein, bacteria often have multiple EIIC proteins, one or more for each carbon source which enters the cell through the PTS (9). Moreover, synthesis of EIIC proteins is typically induced in the presence of its respective carbon source (8). *V. cholerae* contains 25 PTS components, including 13 distinct EIIC domains (10). Recently, the carbohydrate specificity of each EIIC transporter was defined; together, the 13 proteins are able to transport fructose, GlcNAc, (GlcN)₂, glucose, mannitol, mannose, MurNAc, and sucrose into the cell via the PTS (11).

Here, we focus on one of these PTS sugars, fructose. *V. cholerae* is entirely dependent on the PTS system for the uptake of fructose, in contrast to the existence of multiple non-PTS glucose transporters (7, 11). PTS^{Fru}-specific components in *V. cholerae* are encoded by genes located at two distinct loci. First, VC1826 encodes an EIABC fusion protein that is capable of both fructose and mannose transport (7, 11). VCA0516, VCA0517, and VCA0518 make up the second locus encoding PTS^{Fru} proteins (12). VCA0518 (*fruB*) encodes the fructose-specific EIIC domain and FPr, which exist as fusion proteins. VCA0517 (*fruK*) encodes 1-phosphofructokinase, which is responsible for phosphorylating fructose-1-phosphate to fructose-1,6-bisphosphate following uptake and phosphorylation of fructose into the cell. VCA0516 (*fruA*) encodes the fructose-specific EIIB and EIIC domains, which exist as fusion proteins. Experimental evidence suggests that in *V. cholerae*, the proteins encoded by *fruBKA* play the primary role in fructose transport and that FPr is preferred over HPr in PTS transport and phosphorylation of fructose (7, 11).

Relevant to the life cycle of *V. cholerae*, *fruB* (encoding EIIC-FPr, herein shorted to FPr), along with other PTS components, is upregulated when the bacteria enter their viable but nonculturable state, suggesting that the uptake of specific carbon sources may be important for the survival of these bacteria (13). *fruB* is also induced during infection of a mouse model of cholera, and Δ *fruB* mutants demonstrated a 3-fold defect during a colonization assay of infant mice (14). FPr and HPr, moreover, are involved in a signaling cascade that allows the phosphorylation state of EI to impact biofilm formation in growth conditions involving glucose (7). Thus, FPr, along with other PTS^{Fru} components, may be particularly important as *V. cholerae* transitions between environments containing high or low concentrations of fructose. A clearer understanding of *fruB* expression and its regulation in response to changes in carbon source availability would shed light on the persistence of the pathogen.

Here, we investigated the roles of two global transcription factors, Cra and cAMP receptor protein (CRP), in regulating *fruB* expression in *V. cholerae* in various carbon sources. We demonstrate that Cra represses *fruB* transcription in the absence of fructose, likely by acting near the -10 hexamer of the *fruB* promoter, while CRP activates *fruB* expression in the absence of glucose, working farther upstream in the promoter. Our data indicate that the two regulators can work independently to control the production of FPr depending on carbon source availability, although CRP can repress *cra* expression in some growth conditions.

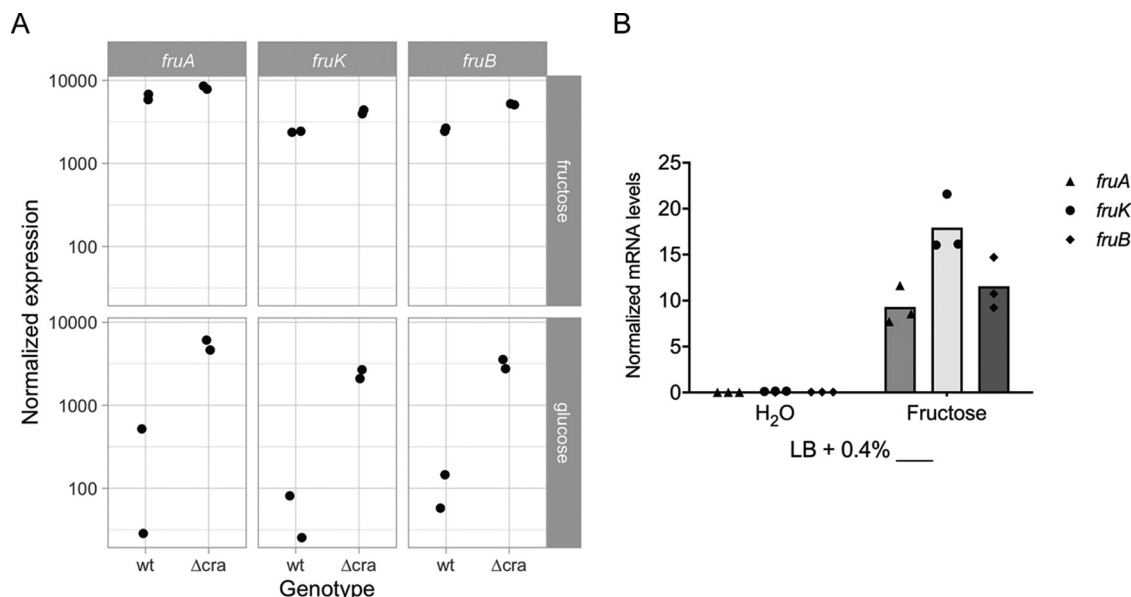


FIG 1 *fruBKA* expression is induced by fructose. (A) Normalized counts for *fruA*, *fruK*, and *fruB* transcripts in wild-type (wt) and Δ cra strains in fructose and glucose growth conditions. RNA for RNA-Seq was extracted from bacteria cultured in 1× M9 supplemented with 0.4% (wt/vol) fructose or glucose and grown to an OD_{600} of ~0.3. (B) *fruA*, *fruK*, and *fruB* expression in a wild-type strain grown in LB supplemented with 0.4% (wt/vol) fructose or an equivalent volume of water. Cultures were grown to an OD_{600} of ~0.3, and then RNA was extracted, purified, and treated with DNase I. qRT-PCR was performed on each total RNA sample using SYBR green and gene-specific primers. RNA amounts were determined using standard curves and then normalized to an endogenous control (4.5S RNA). Bars represent means from biological replicates.

RESULTS

Identification of the *fruB* transcription start site. Before beginning to dissect how *fruB* is regulated, we first confirmed that *fruB*, *fruK*, and *fruA* are all induced by the presence of fructose using a combination of transcriptome sequencing (RNA-Seq) and quantitative reverse transcription-PCR (qRT-PCR). RNA for RNA-Seq was extracted from wild-type (WT) *V. cholerae* cultured in 1× M9 medium supplemented with either fructose or glucose. As expected, given the locus encodes components of PTS^{Fru}, *fruB*, *fruK*, and *fruA*, transcript levels were all higher in the presence of fructose than glucose (Fig. 1A). Moreover, normalized expression of each gene in the *fru* locus showed similar levels of upregulation in fructose as glucose growth conditions, which could suggest coregulation of the three genes. To confirm these results, *fruBKA* transcript levels were also investigated by qRT-PCR. Total RNA was extracted from a WT strain cultured in Luria-Bertani (LB) broth only or LB broth supplemented with fructose. Similar to our RNA-Seq results, all three transcripts were expressed at high levels in fructose medium, and transcript levels decreased in the absence of fructose (Fig. 1B). From both RNA-Seq and qRT-PCR data, we concluded that *fruB*, *fruK*, and *fruA* are each induced and upregulated in fructose medium. A more thorough analysis of the RNA-Seq data, which was done as part of a larger study, will be presented elsewhere.

We then set out to determine the transcription start site (TSS) of *fruB* using 5' RACE (rapid amplification of cDNA ends) (15). RNA was extracted from a WT strain cultured in minimal medium supplemented with fructose, and a primer annealing to the *fruB* coding region was used to reverse transcribe extracted RNA (see Fig. S1 and Table S2 in the supplemental material). cDNA fragments were then amplified and sequenced. Out of 24 total sequences analyzed across 2 separate 5' RACE experiments, we observed the *fruB* TSS (notated as *fruB* TSS-2) to lie 133 nucleotides (nt) upstream of the *fruB* start codon in 5 sequences (position +109 relative to TSS-1, described below; Fig. 2; Fig. S1 and S2). In the 19 remaining samples, we were unable to determine the *fruB* TSS because reverse transcription of *fruB*'s 5' untranslated region (UTR) stopped

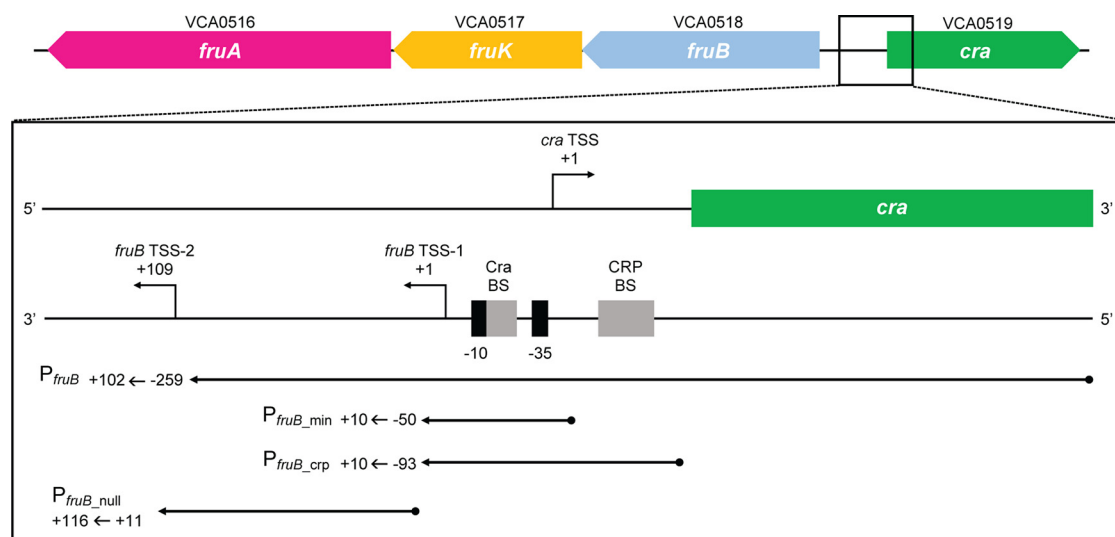


FIG 2 Map of the *fruBKA* locus and *fruB* promoter transcriptional fusions. VCA0518, VCA0517, and VCA0516 (*fruB*, *fruK*, and *fruA*, respectively) encode components of the fructose-specific PTS in *V. cholerae*. VCA0519 (*cra*) encodes a putative transcriptional repressor. The *fruB* transcription start site (TSS) determined by Papenfort et al. is labeled as *fruB* TSS-1 and was designated the +1 site (16). Based on this numbering scheme, the *fruB* start codon begins at position +242. *fruB* TSS-2 was determined by 5' RACE in this work (see Fig. S1 and S2 in the supplemental material). P_{fruB} , P_{fruB_min} , P_{fruB_crp} , and P_{fruB_null} reporters contain portions of the *fruB* promoter indicated by single-headed arrows fused to the 5' end of the *E. coli* *lacZ* gene. Reporters were then inserted into the *lacZ* gene in the *V. cholerae* genome to disrupt endogenous *lacZ* expression. Exact coordinates included in each fusion are listed next to the respective arrow. Putative -10 and -35 sites in the *fruB* promoter are depicted by black bars. Putative binding sites (BSs) for Cra and CRP are depicted by gray bars.

prematurely downstream of the *fruB* start codon. We also performed 5' RACE with RNA extracted from a WT strain cultured in minimal medium supplemented with glucose, using the same workflow. In glucose medium, we observed the *fruB* TSS to lie in roughly the same location as in fructose growth conditions, 133 nt upstream of the *fruB* start codon, in 5 of 12 sequences analyzed (Fig. S3). As in fructose medium, failed reverse transcription reactions prevented us from determining the TSS in all 12 samples. The similarities between our 5' RACE results from fructose and glucose media suggest the location of the *fruB* TSS is not dependent on carbon source when samples are grown in minimal media.

Interestingly, the TSS identified here (*fruB* TSS-2) differs from the TSS identified by Papenfort et al. (notated as *fruB* TSS-1), who reported the *V. cholerae* *fruB* TSS to be 241 bp upstream of the *fruB* start codon (108 nt upstream of TSS-2) (Fig. 2) (16). In their work, Papenfort and colleagues used differential RNA sequencing (dRNA-Seq) to identify TSSs throughout the *V. cholerae* genome (16). RNA used in dRNA-Seq was extracted from WT strains cultured in LB without additional carbon sources present (16). It is possible that differences in minimal versus rich media affect the site of transcription initiation. Analysis of our RNA-Seq data points to the 5' end of *fruB* ranging from roughly the +24 to +74 sites, relative to TSS-1. Therefore, it is also possible that posttranscriptional processing of *fruB* transcripts may occur.

To reconcile the difference between *fruB* TSS-1 and TSS-2, we constructed the P_{fruB} transcriptional reporter, which contains a portion of the *fruB* promoter region fused to the 5' end of the *Escherichia coli* *lacZ* gene (Fig. 2). This construct was then inserted into the middle of the *V. cholerae* *lacZ* homolog in the *V. cholerae* genome to produce the final reporter strain. Through this method, the *V. cholerae* *lacZ* homolog is rendered inert, and all β -galactosidase activity from the LacZ protein, which reflects transcriptional activity, originates from the promoter region included in the reporter. The portion of the *fruB* promoter included in P_{fruB} spans the region from -259 to $+102$, where +1 is *fruB* TSS-1. Notably, the P_{fruB} reporter includes *fruB* TSS-1 identified by Papenfort and colleagues (i.e., the +1 site) and stops 7 nt before the +1 site of *fruB* TSS-2, which

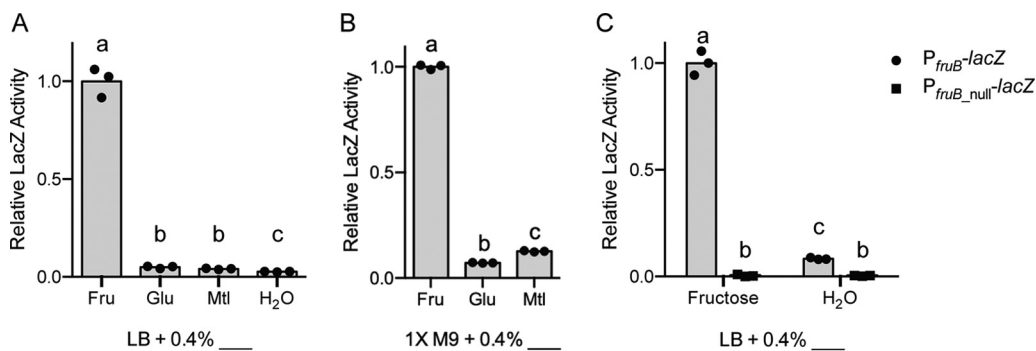


FIG 3 Transcriptional reporter for *fruB* expression. *fruB* promoter activity from the P_{fruB} -*lacZ* transcriptional reporter (A and B) or P_{fruB} -*lacZ* and P_{fruB_null} -*lacZ* transcriptional reporters (C) in the indicated carbon sources relative to activity from the P_{fruB} -*lacZ* reporter in fructose conditions (“relative LacZ activity”). Bacteria were initially cultured in LB (A and C) or 1X M9 plus 0.4% (B) maltose overnight and back diluted into fresh media supplemented with the indicated carbon sources the following day. After reaching an OD_{600} of 1.0, cultures were lysed and incubated with ONPG substrate solution for 1 h, from which A_{420} /minute was measured and normalized to OD_{600} . A baseline value was obtained by averaging all three replicates from the P_{fruB} -*lacZ* reporter in fructose conditions. Relative LacZ activity for other conditions and reporters was calculated by dividing the mean A_{420} /(minute \times OD_{600}) value by the baseline, which was set to 1. For each carbon source, cultures were grown in biological triplicate and measured in technical triplicate. Technical triplicates were averaged during data analysis. Bars represent means from biological triplicates. Within each panel, bars with different letters indicate mean values that are significantly different from each other ($P < 0.05$, Tukey’s multiple-comparison test).

we identified through 5’ RACE (i.e., the +109 site [Fig. 2]). Despite our 5’ RACE data, we postulated that TSS-1 was the more likely start site, as it was the only one of the two that had an identifiable -10 site, which was predicted using BPROM and PromoterHunter and previously determined consensus matrices from both *E. coli* and *V. cholerae* (16–18). Using LacZ assays, we then measured transcriptional activity from the P_{fruB} reporter in a number of PTS carbon sources in both rich (LB) and minimal (M9) media. In both rich and minimal media, we observed the largest amount of β -galactosidase activity (“LacZ activity”) when the medium was supplemented with fructose (Fig. 3A and B). In media supplemented with glucose, mannitol, or, as a control, water, LacZ activity from the P_{fruB} reporter was statistically lower than with fructose as the added carbon source ($P < 0.05$, Tukey’s multiple-comparison test). These results indicate that the P_{fruB} reporter contains at least one intact TSS, as well as a corresponding transcriptional promoter. The P_{fruB} reporter must also contain regions responsible for regulation of *fruB* expression, allowing for at least 8-fold (and up to 37-fold) induction in the presence of fructose (Fig. 3A and B).

In addition to the P_{fruB} reporter, we also constructed the P_{fruB_null} reporter, which spans +11 to +116 of the *fruB* promoter region (Fig. 2). The P_{fruB_null} reporter lacks *fruB* TSS-1 but includes putative -10 and -35 hexamers and the +1 site for *fruB* TSS-2. When we measured LacZ activity, we observed a significant difference in transcriptional activity between the P_{fruB_null} and P_{fruB} reporters in both of the tested growth conditions ($P < 0.05$, Tukey’s multiple-comparison test) (Fig. 3C). Furthermore, no significant difference was observed when comparing transcriptional activity from the null reporter in fructose and water growth conditions. These results suggest the P_{fruB} reporter contains elements necessary for transcription—and induction in the presence of fructose—while the P_{fruB_null} reporter lacks such sites. We concluded that *fruB* TSS-1, and not *fruB* TSS-2, is the point at which *fruB* transcription begins.

***fruB* expression is fine-tuned by available carbon sources.** To further probe the dependence of *fruB* expression on the presence of fructose, we conducted LacZ assays with the P_{fruB} reporter in which cultures were prepared with a mixture of carbon sources, combining fructose and either glucose or mannitol in a range of concentrations. In mixtures of fructose and glucose, LacZ activity from the P_{fruB} reporter decreased 4-fold when an equal amount of glucose (0.2% wt/vol of 0.4% wt/vol total supplemental

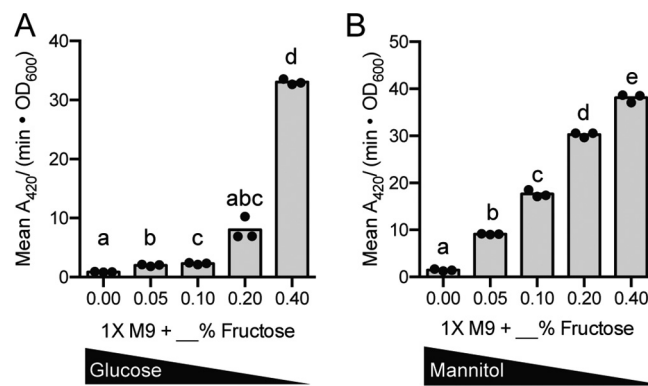


FIG 4 *fruB* expression is carbon source dependent. *fruB* promoter activity in a mixture of carbon sources as measured by mean $A_{420}/(\text{min} \cdot \text{OD}_{600})$ from the P_{fruB} -*lacZ* transcriptional fusion. Bacteria were initially cultured in 1X M9 plus 0.4% maltose overnight and back diluted into fresh media supplemented with the indicated percentage (wt/vol) of fructose and brought to a total 0.4% (wt/vol) sugar with additional glucose (A) or mannitol (B). After reaching an OD_{600} of 1.0, cultures were lysed and incubated with ONPG substrate solution for 1 h, from which A_{420}/min was measured and normalized to OD_{600} . For each carbon source, cultures were grown in biological triplicate and measured in technical triplicate. Technical triplicates were averaged during data analysis. Bars represent means from biological triplicates. Within each panel, bars with different letters indicate mean values that are significantly different from each other ($P < 0.05$, Tukey's multiple-comparison test).

sugar) was included in the culture ($P < 0.05$, Tukey's multiple-comparison test) (Fig. 4A). In mixtures of fructose and mannitol, LacZ activity from the P_{fruB} reporter followed a more linear pattern (Fig. 4B). As a higher percentage of mannitol was included in cultures, LacZ activity significantly decreased ($P < 0.05$, Tukey's multiple-comparison test), although the fold activity reductions were not as high as observed in cultures containing mixtures of fructose and glucose. Similar patterns were observed in analogous Western blots (Fig. S4). These patterns are likely due to the preference for glucose over other carbon sources in bacterial metabolism; in Gram-negative bacteria, carbon catabolite repression regulates metabolic pathways to promote the breakdown of desirable sugars like glucose before others like fructose and mannitol (8, 9, 19). Regardless of carbon source preference, these LacZ assays illustrate the dependence of *fruB* expression on the presence of fructose: a higher percentage of fructose in the system correlates with higher *fruB* expression.

***fruB* expression is regulated by Cra and CRP.** We next turned our attention to identifying the protein regulators that control induction of *fruB* expression in the presence of fructose. Observations from other Gram-negative bacteria provided a starting point from which to evaluate possible regulators of *fruB* in *V. cholerae*. Lying directly adjacent to the *fruBKA* locus in *V. cholerae*, VCA0519 encodes a LacI-GalR family transcriptional regulator referred to both as FruR (fructose repressor) and Cra (catabolite repressor/activator) (Fig. 2) (12). In *E. coli*, Cra is considered a global transcriptional regulatory protein that affects the metabolism of 36 different carbon sources and represses *fruB* expression (20–24). Alongside Cra, the 3',5'-cyclic AMP (cAMP) receptor protein (CRP) is another global regulator that affects *fruB* expression in *E. coli* and *Salmonella enterica* serovar Typhimurium by activating the gene's transcription (25, 26). In *V. cholerae*, moreover, a *crp* mutant strain exhibited decreased expression of *fruB* and *fruA*, along with decreased fructose metabolism (27, 28).

We first investigated Cra as a potential regulator of *fruB* in *V. cholerae*. We repeated our RNA-Seq analysis using a Δ cra mutant. In the absence of *cra*, expression of all three transcripts increased in glucose medium, indicating that Cra represses *fruB*, *fruK*, and *fruA* expression in the presence of glucose and providing preliminary evidence that Cra represses *fruB* in nonfructose media (Fig. 1A). To further examine this relationship, we evaluated FPr protein levels in WT and Δ cra strains in fructose, glucose, and

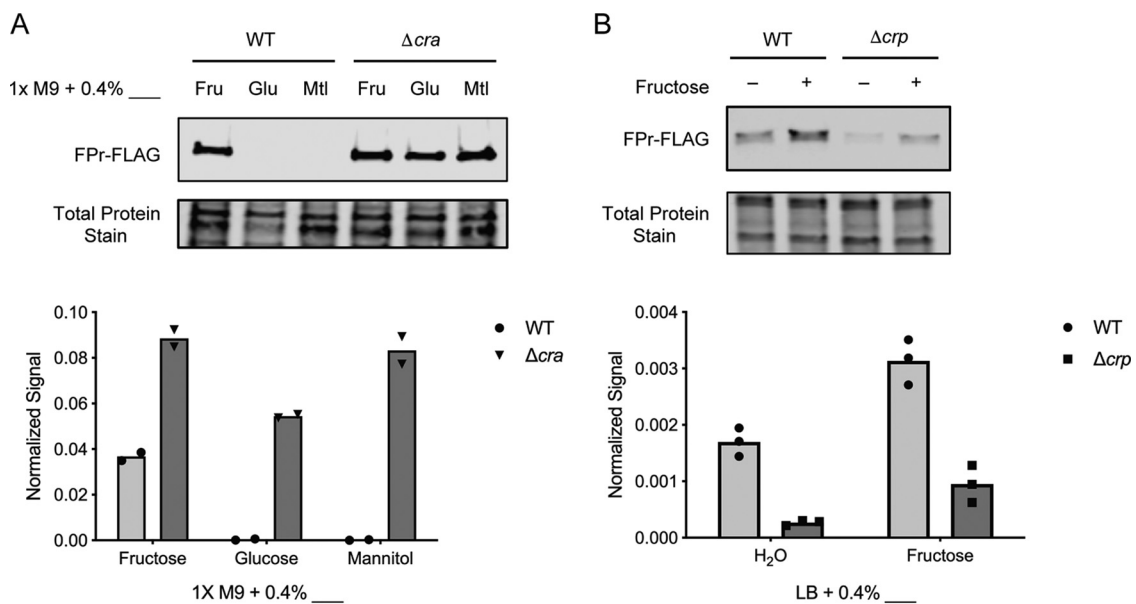


FIG 5 FPr levels are regulated by Cra and CRP. Western blotting of FPr-FLAG in wild-type and Δ cra (A) or Δ cpr (B) strains. Strains were cultured in 1x M9 supplemented with 0.4% (wt/vol) fructose (Fru), glucose (Glu), or mannitol (Mtl) (A) or LB supplemented with 0.4% (wt/vol) fructose (+fructose) or an equivalent volume of water (−fructose) (B). Once cultures reached late log phase, total cell lysate was extracted and run on an SDS-PAGE gel, and anti-FLAG antibodies were used to probe for FLAG-tagged FPr. FPr levels were quantified using LiCor Image Studio and normalized to total protein levels. Bars represent means from biological replicates. In panel B, both pairwise differences comparing WT and Δ cpr were significant at $P < 0.05$ (Sidak's multiple-comparison test).

mannitol growth conditions (Fig. 5A). Similar to the expression patterns observed in our RNA-Seq results, FPr levels were highest in media supplemented with fructose and decreased 100-fold in nonfructose media. In the absence of cra, FPr levels increased compared to the WT strain across all culture conditions, supporting the role of Cra as a repressor of *fruB* in nonfructose media. Moreover, these data provide additional evidence that the transcriptional regulator Cra specifically affects *fruB* transcription and such effects are reflected at the protein level as well.

We also evaluated the relationship between CRP and FPr, given evidence which implicates CRP as an activator of *fruB* expression (27, 28). To do so, we measured FPr levels in WT and Δ cpr strains when LB cultures were supplemented with fructose or an equivalent volume of water (Fig. 5B). Consistent with our previous findings, FPr levels were highest in cultures supplemented with fructose. In the absence of CRP, FPr levels in both fructose and nonfructose conditions decreased 3- to 6-fold ($P < 0.05$, Sidak's multiple-comparison test), suggesting that CRP activates *fruB* expression in both growth conditions.

To confirm that Cra and CRP are regulators of *fruB* transcription, we used the P_{fruB} reporter to measure *fruB* expression in a series of LacZ assays. In these assays, we measured LacZ activity from the P_{fruB} reporter in strains lacking either the endogenous *cra* or *cpr* loci. In an effort to probe Cra- and CRP-mediated *fruB* regulation independently, these strains (herein referred to as "mutant strains") also lacked the endogenous locus of the other regulator (i.e., the *cra* mutant strain also lacked the endogenous *cpr* locus and was compared to a strain that possessed *cra* but still lacked *cpr*). To rule out polar effects, we also measured LacZ activity from a complementation strain that possessed a plasmid containing the *cra* or *cpr* gene under the control of an inducible promoter (pJML05::*cra* or pTrc99A::*cpr*).

In assessing the activity of Cra, the deletion of *cra* resulted in 2- and 38-fold increases in LacZ activity when the strains were grown in fructose and nonfructose media, respectively ($P < 0.05$ by Tukey's multiple-comparison test) (Fig. 6A). In both

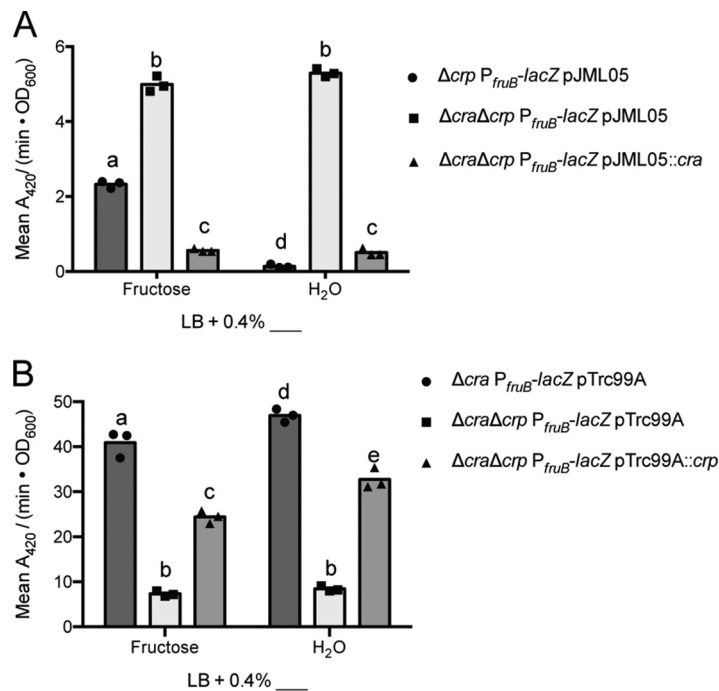


FIG 6 Cra represses *fruB* expression, while CRP activates *fruB* expression. *fruB* promoter activity from the P_{fruB} transcriptional reporter upon reintroduction of *cra* (A) or *crp* (B) expression via the pJML05::*cra* or pTrc99A::*crp* plasmids or the corresponding empty vectors in Δ *cra*, Δ *crp*, or Δ *cra* Δ *crp* strains. Strains were initially grown solely in LB and back-diluted into fresh cultures supplemented with 0.4% (wt/vol) fructose or an equivalent volume of water. Strains harboring the pJML05 vector or a derivative were also supplemented with 5 mM IPTG, while strains harboring the pTrc99A vector or a derivative were supplemented with 1 mM IPTG. After reaching an OD_{600} of 1.0, cultures were lysed and incubated with ONPG substrate solution for 1 h, from which A_{420}/minute was measured and normalized to OD_{600} . For each carbon source and strain, cultures were grown in biological triplicate and measured in technical triplicate. Technical triplicates were averaged during data analysis. Bars represent means from biological replicates. Within each panel, bars with different letters indicate mean values that are significantly different from each other ($P < 0.05$, Tukey's multiple-comparison test).

growth conditions, LacZ activity in the complementation strain (Δ *cra* Δ *crp* P_{fruB} -*lacZ* pJML05::*cra*) was significantly less than LacZ activity in the mutant strain containing an empty vector (Δ *cra* Δ *crp* P_{fruB} -*lacZ* pJML05; $P < 0.05$ by Tukey's multiple-comparison test) (Fig. 6A). We conclude that Cra represses *fruB* expression by directly or indirectly affecting some portion of the *fruB* promoter included in the P_{fruB} reporter.

The *crp* mutant strain, on the other hand, produced 5-fold lower LacZ activity ($P < 0.05$, Tukey's multiple-comparison test) in both fructose and nonfructose growth conditions compared to the "WT strain" containing the endogenous *crp* locus (Fig. 6B). Also in both growth conditions, LacZ activity in the complementation strain (Δ *cra* Δ *crp* P_{fruB} -*lacZ* pTrc99A::*crp*) was 3-fold higher than the mutant strain containing an empty vector (Δ *cra* Δ *crp* P_{fruB} -*lacZ* pTrc99A) (Fig. 6B), suggesting partial complementation. Overall, these results support a role for CRP in activating *fruB* transcription in both fructose and nonfructose conditions by acting, directly or indirectly, on some portion of the *fruB* promoter included in the P_{fruB} reporter. Collectively, data presented in Fig. 6 also indicate that Cra and CRP can work independently of the other to regulate *fruB* expression.

Determination of Cra and CRP regulatory sites. Having established Cra and CRP as transcriptional regulators of *fruB* expression using the P_{fruB} reporter, we then constructed additional transcriptional reporter fusions to identify regulatory sites for each regulator in the *fruB* promoter. In constructing these reporters, we considered the locations of putative regulatory sites for Cra and CRP to act directly on the promoter, based

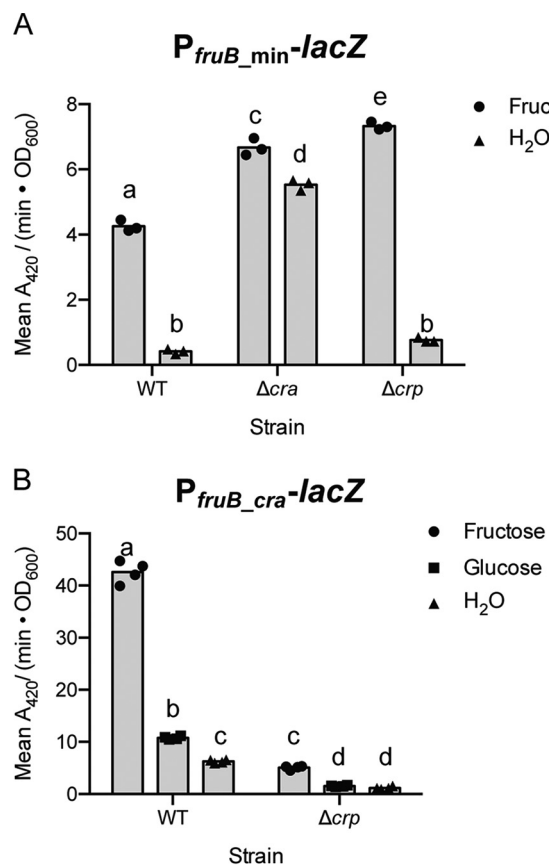


FIG 7 Cra acts near the predicted -10 and -35 sites of the *fruB* promoter, while CRP acts farther upstream. (A) *fruB* promoter activity from P_{fruB_min} transcriptional reporter in wild-type, Δcra , and Δcpr strains. (B) *fruB* promoter activity from P_{fruB_cra} transcriptional reporter in wild-type and Δcpr strains. Strains were initially grown in LB and back diluted into fresh cultures supplemented with 0.4% (wt/vol) fructose, glucose, or an equivalent volume of water. After reaching an OD_{600} of 1.0, cultures were lysed and incubated with ONPG substrate solution for 1 h, from which A_{420}/minute was measured and normalized to OD_{600} . For each carbon source and strain, cultures were grown in biological replicates and measured in technical triplicate. Technical triplicates were averaged during data analysis. Bars represent means from biological replicates. Within each panel, bars with different letters indicate mean values that are significantly different from each other ($P < 0.05$, Tukey's multiple-comparison test).

on computational predictions and their similarities to consensus sequences in *E. coli* and *V. cholerae*. BPROM identified only one putative Cra site starting at position -12 in relation to *fruB* TSS-1 (Fig. 2 and Fig. S1). Moreover, the sequence of this putative site, TGAATC-GATTCA, aligns well with the palindromic Cra consensus sequence previously identified in *E. coli*, TGAAAC-GTTTCA (20–23, 29). To evaluate the validity of this predicted regulatory site, we constructed the P_{fruB_min} reporter, which spans -50 to $+10$ of the *fruB* promoter region and is smaller than the P_{fruB} reporter (Fig. 2). We then measured LacZ activity from the P_{fruB_min} reporter in WT and Δcra strains in rich media supplemented with fructose or, as a control, water. We observed a 10-fold induction of LacZ activity when the P_{fruB_min} reporter strain was grown in the presence of fructose, and this induction was reduced to 1.2-fold when *cra* was absent ($P < 0.05$, Tukey's multiple-comparison test) (Fig. 7A). These observations suggest that the promoter, as well as a TSS, are still intact within the P_{fruB_min} reporter. In the *cra* mutant strain, LacZ activity from the P_{fruB_min} reporter increased in both growth conditions compared to the WT strain ($P < 0.05$, Tukey's multiple-comparison test), indicating that Cra-mediated regulation is still taking place within the 60 nt of the *fruB* promoter included in the P_{fruB_min} reporter and is responsible for the majority of the induction observed from this minimized promoter. This region includes the sequence that spans the predicted -10 and

–35 hexamers, where a transcriptional repressor has the opportunity to enact a large effect on RNA polymerase recruitment or activity (30). We also note that the original P_{fruB} reporter presented a 20- to 37-fold induction upon addition of fructose to the growth medium (Fig. 3A) compared to the 10-fold induction obtained using the P_{fruB_min} construct. Thus, while the P_{fruB_min} -*lacZ* reporter is induced by fructose, P_{fruB_min} may exclude regulatory sites for a transcriptional activator or an additional TSS needed for maximal induction.

We also evaluated the P_{fruB_min} reporter in the context of CRP. LacZ activity from the P_{fruB_min} reporter in a *crp* mutant strain presented 10-fold induction in the presence of fructose, similar to what was observed in the WT strain ($P < 0.05$, Tukey's multiple-comparison test) (Fig. 7A), which suggests that regulatory sites responsive to CRP are not included in the P_{fruB_min} construct. We noted, however, that in fructose-supplemented medium, deletion of *crp* led to a 1.7-fold increase in LacZ activity compared to the WT ($P < 0.05$, Tukey's multiple-comparison test). This is inconsistent with CRP functioning as a transcriptional activator (Fig. 5B and 6B). Our transcriptional reporters are integrated, in an antisense direction, into the native *lacZ* gene in the *V. cholerae* genome, which is activated by CRP (data not shown). We postulate that the observed changes in LacZ activity when comparing P_{fruB_min} in the WT and Δcrp strains in certain growth conditions may represent changes in antisense transcriptional readthrough that become more prominent given the low activity of the P_{fruB_min} construct.

To account for promoter regions through which CRP activates *fruB* expression, we used the search tool Virtual Footprint, which predicted a CRP site lying 61 nt upstream of the *fruB* TSS (TSS-1) (Fig. 2 and Fig. S1) (31). The location of this predicted regulatory site almost perfectly matches the location of the CRP site known to exist in the *E. coli* *fruB* promoter, which lies 60 nt upstream of the *fruB* TSS (25). Additionally, the sequence of this putative site, TGTGC-GTCTGA-TCATA, is in good agreement with the sequence of the CRP box motif previously identified in *E. coli*, TGTGA-NNNNNN-TCACA (25).

To validate or invalidate this predicted site, we constructed the P_{fruB_crp} reporter, which spans –93 to +10 of the *fruB* promoter and includes the predicted CRP box (Fig. 2). We then measured LacZ activity from this reporter in WT and Δcrp strains (Fig. 7B). Consistent with our assessment that CRP is an activator of *fruB*, across all culture conditions, LacZ activity from the P_{fruB_crp} reporter decreased significantly in the *crp* mutant strain compared to the WT ($P < 0.05$, Tukey's multiple-comparison test). Also, even in the absence of *crp*, the addition of fructose to the growth medium induced LacZ activity 3- to 4-fold, compared to 4- to 7-fold in the WT ($P < 0.05$, Tukey's multiple-comparison test). This change in fold induction likely represents the loss of the activator, CRP, but maintenance of the repressor, Cra. Collectively, LacZ activity from both P_{fruB_min} and P_{fruB_crp} reporters allows us to narrow the location of a putative CRP binding site to a 43-nt region that lies within the region of *fruB* promoter included in the P_{fruB_crp} reporter but excluded from the P_{fruB_min} reporter.

CRP represses *cra* expression. In the above-described assays, we established that Cra and CRP affect *fruB* expression in the absence of the other regulator (Fig. 6). However, these assays fail to consider the possibility that the two regulators also interact in modulating *fruB* expression. The CRP binding site predicted by Virtual Footprint, which lies in the *fruB*-*cra* intergenic region, resides in close proximity to the *cra* TSS lying on the opposite strand (Fig. 2). To test whether the expression of *cra* is dependent on CRP, we constructed a transcriptional reporter containing the *cra* promoter region (Fig. S5 and S6). We then measured LacZ activity from the P_{cra} reporter in WT and Δcrp strains in LB containing fructose, glucose, mannitol, or, as a negative control, water (Fig. 8). In both mannitol and negative-control conditions, no significant changes in LacZ activity between strains were observed ($P > 0.05$, Sidak's multiple-comparison test) (Fig. 8). In both fructose and glucose conditions, however, we observed significant increases in LacZ activity in the *crp* mutant strain compared to WT, which suggests that CRP may repress *cra* expression in the presence of these carbon sources. We

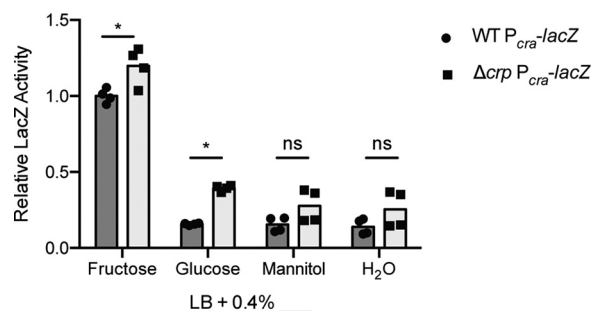


FIG 8 CRP represses *cra* expression in fructose and glucose growth conditions. *cra* promoter activity in multiple carbon sources in the presence and absence of CRP as measured by mean A_{420} /minute from the $P_{cra}-lacZ$ transcriptional fusion. Strains were initially grown in LB overnight and back diluted into fresh cultures supplemented with 0.4% (wt/vol) fructose, glucose, mannitol, or an equivalent volume of water the following day. After reaching an OD_{600} of 1.0, cultures were lysed and incubated with ONPG substrate solution for 1 h, from which A_{420} /minute was measured and normalized to OD_{600} . A baseline value was obtained by averaging all replicates from the WT $P_{cra}-lacZ$ reporter in fructose conditions. Relative LacZ activity for other conditions and reporters was calculated by dividing the mean A_{420} /(minute $\times OD_{600}$) value by the baseline, which was set to 1. For each carbon source, cultures were grown in biological replicate and measured in technical triplicate. Technical triplicates were averaged during data analysis. *, pairwise differences when comparing different strains in the same carbon source were significant at $P < 0.05$; ns, not significant (Sidak's multiple-comparison test).

postulate that in the presence of fructose, CRP prevents unnecessary, excess synthesis of Cra, and in glucose conditions, CRP may “rein” in Cra to allow for some basal levels of FPr to be synthesized such that the bacteria are primed to metabolize fructose once it is available.

DISCUSSION

Important to the survival of *V. cholerae* is its ability to respond to changes in carbohydrate availability, depending on its current environment (7). The series of carbohydrate-specific PTSs encoded in the *V. cholerae* genome is believed to be crucial to this process; PTS components are thought to be selectively produced in order to transport and phosphorylate available carbon sources into the bacteria for metabolism (7, 10, 11). Here, we describe the transcriptional regulation of *fruB*, which encodes the FPr component of PTS^{Fru}, in an effort to further dissect how *V. cholerae* responds to changes in carbohydrate availability. We show that *fruB* is expressed at the highest levels in fructose media, which is consistent with data collected during a similar study in *Pseudomonas putida*, the only other Gram-negative bacterium that, to our knowledge, has been used to study *fruB* using a transcriptional reporter system (32). Expression of *fruB* is controlled by both Cra and CRP, which impact transcription through different regions of the *fruB* promoter in response to the absence and presence of fructose. The proximal location of *fruK* and *fruA* to *fruB*, and their parallel induction by fructose, further suggests that the three genes may be coregulated by Cra and CRP.

Using the P_{fruB} reporter, we showed that the *fruB* TSS lies approximately 241 nt upstream of its start codon, in line with previously published dRNA-Seq data from Papenfort and colleagues (Fig. 2 and 3; see Fig. S1 in the supplemental material) (16). This conflicts with the TSS we determined by 5' RACE, which lies 133 nt upstream of the *fruB* start codon (Fig. 2; Fig. S1 and S2). Interestingly, the intergenic transcript IGR4 (107 nt) lies directly between these two sites, spanning almost the entire length between the two markers (Fig. S1). IGR4 was first identified in a massively parallel sequencing experiment which aimed to uncover novel small RNAs (sRNAs) with regulatory roles in *V. cholerae* (33). Because of its proximity to the *cra* promoter region, IGR4 was hypothesized to be a putative *cis*-acting sRNA, imparting regulation through extensive binding to the *cra* promoter (34). However, Western blotting probing for Cra in a strain overexpressing IGR4 suggests the small transcript has no regulatory effect on Cra levels (Fig. S7). One possible explanation for the range of 5' ends observed in

our RNA-Seq data, our aberrant 5' RACE results, as well as the existence of IGR4, is the occurrence of posttranscriptional processing of the *fruB* transcript by an endonuclease. RNase E, arguably the most prominent RNase in *E. coli*, and YbeY are both promising candidates for cleavage of *fruB* mRNA; these two endonucleases have also been shown to target transcripts in *V. cholerae* (35–38).

Using P_{fruB_min} and P_{fruB_crp} reporters, we identified sites through which Cra and CRP influence *fruB* transcription, possibly through direct interactions with the *fruB* promoter; the likely locations of –10 and –35 hexamers of the *fruB* promoter were also mapped (Fig. 7A and B). The sequences of predicted regulator binding sites identified here agree well with previously determined consensus sequences from *E. coli* (Fig. S1) (20–23, 25, 29). In the *V. cholerae* genome, the –10 hexamer shows a distinct consensus sequence, TAnaAT (spanning –12 to –7 sites), and highly conserved bases at positions –11 and –7 (adenine and thymine, respectively) are maintained in the sequence of the –10 hexamer we predict here, CAGTAT (16). While the manuscript was under review, a separate study was published that demonstrated the binding of Cra to the putative Cra binding site we included in the P_{fruB_min} -*lacZ* construct (Fig. 2 and Fig. S1) (39). Interestingly, the authors propose that in some growth conditions, Cra may recruit RNA polymerase to the *fruB* promoter (39). These results, combined with those presented in this work, open up intriguing possibilities for further interrogation of the nuances of *fruB* expression throughout the *V. cholerae* life cycle.

In *E. coli*, Cra is frequently described as a pleiotropic regulator, involved in modulating the expression of a large number of genes, including *mtlA*, which encodes the EII^{Mtl} protein (22). While Cra-mediated repression of the *fru* operon in *V. cholerae* closely mimics the same process in *E. coli*, it is unclear if a similar Cra regulon exists in *V. cholerae*. Western blotting probing for the PTS^{Mtl} transporter MtlA in WT and Δcra strains suggests the *V. cholerae* Cra regulon may not include the same targets as in *E. coli*; MtlA levels did not vary between WT and mutant strains in *V. cholerae*, although Cra has been shown to repress MtlA in *E. coli* (20) (Fig. S8). Our RNA-Seq data further confirm this finding. Thus, although Cra regulates *fruB* expression in both *E. coli* and *V. cholerae*, their regulons likely contain divergent targets.

One peculiarity in our description of Cra's activity in the *fruB* promoter is the repressor's individual expression pattern. LacZ activity from the P_{cra} reporter and analogous Western blotting probing for Cra indicate that *cra* is expressed at the highest levels in fructose media, just like *fruB* (Fig. 8 and Fig. S8), and in the absence of fructose, Cra levels are low. This particular expression pattern is not intuitive given our observations of Cra activity. In fructose media, Cra is expressed at the highest levels when its activity as a repressor is expected to be minimal. In nonfructose media, Cra is expressed at much lower levels but is active in repressing *fruB*. Similar patterns of expression and activity have been observed in *V. cholerae* for the transcriptional regulator MtlR, which represses the genes encoding PTS^{Mtl} in the absence of the sugar alcohol mannitol (40). In the case of Cra, fructose-1-phosphate (F1P) may provide an explanation for these unexpected activity patterns. We propose a model that when fructose is imported into the cell, it is first phosphorylated to F1P as it crosses the inner bacterial membrane and is then phosphorylated again once inside by 1-phosphofructokinase (the protein product of *fruK*) to become fructose-1,6-bisphosphate (FBP) (12). In *E. coli*, F1P has been shown to bind Cra and significantly inhibit Cra's DNA binding ability (41). Considering the similarities between *E. coli* *cra* and its *V. cholerae* homolog, we hypothesize F1P likely plays a similar role in *V. cholerae* and could help to explain why Cra is inactive in fructose media, even when expressed at relatively high levels. The enzymatic activity of FruK, which converts F1P to FBP, may initiate a feedback loop that controls Cra activity; FruK's activity essentially removes the effector molecule (i.e., F1P) which dampens Cra activity. When the concentration of F1P decreases, Cra becomes active and represses *fruB* transcription, which may, in turn, also decrease expression of *fruK*, consequently increasing the concentration of F1P. As this concentration increases, Cra becomes inactive, *fruB* expression increases, and the cycle repeats itself.

MATERIALS AND METHODS

Strains and culture conditions. All strains used in this study are described in Table S1 in the supplemental material. The wild-type *V. cholerae* strain used in this study, from which all subsequent strains were constructed, was the O1 biovar El Tor N16961 Δ *tcpA* strain. The *tcpA* mutant is highly attenuated for virulence and was used for safety purposes. Unless otherwise denoted, “wild type” refers to the N16961 Δ *tcpA* strain.

All strains were streaked onto Luria-Bertani (LB) plates with the appropriate antibiotics and incubated at 37°C for 12 to 16 h. Liquid cultures were prepared by inoculating 2 ml LB broth or 1 \times M9 minimal medium containing one or more carbon sources (totaling 0.4% [wt/vol]) with individual colonies. All cultures were supplemented with the appropriate antibiotics at the following concentrations: streptomycin (Sm) at 100 μ g/ml and carbenicillin (Cb) at 50 to 100 μ g/ml. Cultures prepared in 1 \times M9 minimal medium were also supplemented with 0.1% (wt/vol) trace metals (5% MgSO₄, 0.5% MnCl₂, 0.5% FeCl₃, and 0.4% nitrilotriacetic acid). Unless otherwise stated, cultures were incubated at 37°C for 12 to 16 h, with shaking at 250 rpm.

Mutant strain construction. *V. cholerae* strains harboring chromosomal mutations were constructed as follows. A plasmid bearing the desired mutation was constructed in the allelic exchange vector pCVD442 via splicing by overlap extension (SOE) PCR. Two roughly 600-bp DNA fragments flanking the region of interest were amplified by PCR using F1/R1 and F2/R2 primer pairs (Table S2). These fragments were annealed together and then amplified by PCR using the F1 and R2 primers. The final PCR product was assembled via Hi-Fi DNA assembly (New England BioLabs) with the pCVD442 backbone, which was prepared using the appropriate pCVD_F and pCVD_R primers (Table S2). The resultant plasmid was propagated in *E. coli* DH5 α pir and then transformed into *E. coli* SM10 λ pir before being conjugated into *V. cholerae*. Successful conjugates were selected from one round of growth in LB broth with streptomycin, and the resultant colonies were plated on sucrose medium to screen for successful vector disintegration. Sucrose-resistant colonies were screened for the desired mutation by PCR with the F0 and R0 primers and confirmed by sequencing (Eurofins).

Transcriptional reporter construction. To assemble the *lacZ* transcriptional fusion reporters, we generated a series of derivatives of the pJL1::*lacZ*(Ec) plasmid, which contains the ribosome binding site (RBS) and coding sequence of *E. coli* *lacZ* [*lacZ*(Ec)] inserted into a fragment of the VC2338 locus (encoding the *V. cholerae* homolog of *lacZ*) in the antisense orientation (42). In each derivative plasmid, we inserted the desired portion of the *fruB* promoter directly upstream of the *lacZ*(Ec) RBS. To construct derivative plasmids for P_{fruB} and P_{fruB_min} reporters, DNA fragments containing the desired portion of the *fruB* promoter were amplified by PCR using forward insert and reverse insert primer pairs (Table S2). The derivative plasmid was then assembled via Hi-Fi DNA assembly (New England BioLabs) with the amplified DNA fragment and the pJL1::*lacZ*(Ec) backbone, which was amplified by PCR using forward vector and reverse vector primers (Table S2). To construct derivative plasmids for P_{fruB_crp} and P_{fruB_null} reporters, desired double-stranded DNA (dsDNA) fragments of the *fruB* promoter (gBlocks) were ordered from Integrated DNA Technologies, and plasmids were assembled via Hi-Fi DNA assembly as described for P_{fruB} and P_{fruB_min} reporters. The exact coordinates of the *fruB* promoter region included in each fusion are indicated in Table S1.

Derivative plasmids were then propagated in *E. coli* DH5 α pir, and correct assembly of the plasmid was checked by sequencing using LIU126 and LIU127 primers, which flank the site at which regions of the *fruB* promoter were inserted into pJL1::*lacZ*(Ec) (Table S2). Plasmids were then transformed into *E. coli* SM10 λ pir before being conjugated into *V. cholerae*, using the sucrose-screening method described above.

Complementation plasmid construction. All plasmids were constructed using the Hi-Fi master mix (New England BioLabs) to assemble DNA fragments. Plasmid pTrc99a::crp was obtained using PCR fragments amplified using primers LIU152-153 (to amplify the pTrc99a backbone) and LIU154-155 (to amplify *crp* from the *V. cholerae* genome). Vector pJML05 was created by replacing the P_{trc} promoter in the pTrc99a backbone with the PLlacO-1 promoter. This was accomplished using primers LIU476-477 to amplify the backbone of pTrc99a and DNA oligonucleotide LIU480. Plasmid pJML05::cra was assembled using PCR products derived by using primers LIU652-653 (to amplify the backbone of pJML05) and LIU654-655 (to amplify *cra* from the *V. cholerae* genome). Plasmid pJML05::IGR4 was assembled from PCR products obtained using primers LIU494-495 (to amplify the backbone of pJML05) and LIU496-497 (to amplify the IGR4 sequence from the *V. cholerae* genome). All constructs were confirmed by sequencing.

RNA-Seq experiments and analysis. For each combination of strain and growth sample, RNA samples in biological duplicate were prepared. Cells from LB agar plates were used to inoculate 2 ml of 1 \times M9 minimal medium supplemented with 0.4% glucose or fructose (wt/vol). Overnight cultures were diluted into 2 ml fresh 1 \times M9 medium with 0.4% glucose or fructose (starting optical density at 600 nm [OD₆₀₀], \sim 0.05) and grown to an OD₆₀₀ of \sim 0.3. The entire culture was harvested (8,000 \times g, 5 min, 4°C), and the RNA was purified from the cells using the Direct-zol RNA miniprep kit (Zymo Research) following the manufacturer's instructions. Eluted samples were treated with DNase at 37°C for 30 min, twice, using Turbo DNA-free (Ambion) according to the manufacturer's protocol. RNA integrity was initially analyzed by agarose gel electrophoresis. Additional RNA integrity analysis, rRNA depletion, cDNA synthesis, and library preparation and sequencing were performed by Quick Biology (Pasadena, CA). Paired-end, 150-bp sequences were generated for 10 million reads per sample.

Fastq files were mapped to the *V. cholerae* biovar El Tor strain N16961 genome (NCBI accession no. GCA_000006745.1) using the BWA-MEM algorithm in BWA version 0.7.12 (43). Aligned reads were counted with htseq-count version 0.11.2 (44) with the intersection-strict argument. Counts were

imported into R version 3.6.2 (45), and differential expression was assessed with DEseq2 version 1.26.0 (46).

General total RNA extraction. RNA for 5' RACE and qRT-PCR was extracted from overnight *V. cholerae* cultures that were back diluted and grown to mid-log phase ($OD_{600} \sim 0.3$). Total RNA was extracted using the Direct-zol RNA miniprep kit (Zymo) following the manufacturer's instructions. For qRT-PCR, eluted samples were treated with DNase at 37°C for 30 min using Turbo DNA-free (Ambion) according to the manufacturer's protocol.

qRT-PCR. Determination of relative expression levels was performed on total RNA using the Stratagene MX3005P system, the Brilliant II SYBR green qRT-PCR master mix kit (Agilent), and primers specific to *fruB*, *fruK*, *fruA*, and 4.5S (Table S2 in the supplemental material). The reactions were set up in 96-well optical reaction plates and contained 1× Brilliant SYBR green qPCR master mix, 30 nM ROX reference dye, each primer at 100 nM, 100 ng RNA, and 1 μ l RT/RNase block enzyme mixture in a 25- μ l reaction mixture. The following conditions were used for cDNA synthesis and PCR: 30 min at 50°C, 10 min at 95°C, and 40 cycles of 30 s at 95°C and 1 min at 60°C (Agilent). MxPro QPCR software (v. 4.10) was used to determine threshold cycle (C_T) values for each reaction, and relative RNA concentrations were calculated from the C_T values by comparison to standard curves. All transcript levels were normalized to a 4.5S RNA endogenous control. No signals were detected in no-template controls and no-reverse transcriptase (RT) controls.

5' RACE. 5' rapid amplification of cDNA ends (RACE; Invitrogen) was performed according to the manufacturer's instructions. Gene-specific primers (GSPs) (Table S2) were designed to anneal to the coding region of the gene of interest (i.e., *cra* or *fruB*) in order to synthesize cDNA and amplify the upstream region from extracted RNA samples. Amplified PCR products were introduced into the pCR4-TOPO vector using the TOPO TA cloning kit (Invitrogen). Plasmids were then isolated and sequenced using M13 forward and M13 reverse primers (Eurofins).

Transcriptional reporter assays. All transcriptional reporter assays were performed using strains containing a *lacZ*(Ec) gene construct that was inserted into the endogenous *lacZ* gene in order to disrupt native *lacZ* expression. Bacterial samples were taken from liquid cultures which were back diluted and grown to late log phase ($OD_{600} \sim 1.0$). In strains harboring the pJML05 plasmid or a derivative, 5 mM isopropyl- β -D-thiogalactopyranoside (IPTG) was added to back dilutions to induce expression from the P_{lacO}-1 promoter. In strains harboring the pTrc99a plasmid or a derivative, 1 mM IPTG was added to back dilutions to induce expression from the *trc* promoter. Cell samples (200 μ l) were loaded into a clear 96-well plate in replicate, and OD_{600} measurements were taken using a Synergy 4 plate reader (BioTek). From these samples, 100 μ l of cells were lysed for 25 to 35 min with a 10- μ l solution containing PopCulture reagent (Novagen) and lysozyme (Thermo Fisher) in a 1,000:1 ratio. Samples (30 μ l) of cell lysate were then incubated with 150 μ l of *o*-nitrophenyl- β -D-galactopyranoside (ONPG) substrate solution (60 mM Na₂HPO₄, 40 mM NaH₂PO₄, 1 mg/ml ONPG, and 2.7 μ g/ml β -mercaptoethanol) in a separate 96-well plate at 28°C. The absorbance at 420 nm (OD_{420}) was recorded every 30 s over 60 min by a Synergy 4 plate reader (BioTek). Final results (denoted in the text as LacZ activity) are reported as the average slope (in mean OD_{420} per minute) of the 30-s intervals over the course of the 60-minute incubation period normalized to OD_{600} (mean OD_{420} /[minute \times OD_{600}]). Technical replicates were averaged during data analysis and statistical analyses were performed using GraphPad Prism (version 7) software.

Western blotting. For FPr-FLAG and MtIA-FLAG analysis, cell pellets were prepared from 2 ml back-diluted cultures grown to mid-log phase ($OD_{600} \sim 0.3$). Following centrifugation at 8,000 \times g for 5 min at 4°C, pellets were resuspended in LB or 1× M9 medium, mixed 1:4 in SDS sample buffer (250 mM Tris-HCl [pH 6.8], 10% SDS, 50% glycerol, 10% β -mercaptoethanol, and 0.5% orange G), and heated at 95°C for 10 min. Samples were loaded onto an SDS containing 4 to 20% Tris gel (Bio-Rad) and run at 200 V for 25 min. Proteins were then transferred to a nitrocellulose membrane using a Trans-Blot Turbo transfer system (7 min at 1.3 A; Bio-Rad). Revert total protein stain (Li-Cor), a near-infrared fluorescent membrane stain, was then used to stain all protein on the membrane following the manufacturer's instructions. Revert stain was detected at 700 nm using an Odyssey imager (Li-Cor). The membrane was then incubated with a dilution of primary antibody (1:5,000 of rabbit anti-FLAG [Abcam]) for 1 h, followed by incubation with a dilution of secondary antibody (1:10,000 of IR800-conjugated goat anti-rabbit immunoglobulin [Li-Cor]) for 30 min. Signal was visualized at 800 nm using an Odyssey imager (Li-Cor), and ImageStudio software (version 5; Li-Cor) was used to quantify fluorescent signal and normalize values to Revert total protein measurements.

For Cra-hemagglutinin (HA) analysis, cell pellets were prepared from 50-ml back-diluted cultures grown to mid-log phase ($OD_{600} \sim 0.3$). Pellets were lysed with B-PER bacterial protein extraction reagent (Thermo Scientific) in the presence of DNase I (Thermo Scientific) following the manufacturer's instructions. Following protein extraction, the same methods used for FruB-FLAG and MtIA-FLAG analysis (described above) were used. During the immunodetection steps, membranes were incubated with rabbit anti-HA antibody (Abcam) in a 1:1,000 dilution for 1 h, followed by a 30-minute incubation with IR800-conjugated goat anti-rabbit (Li-Cor) antibody in a 1:6,667 dilution.

Data availability. RNA-Seq data were deposited in the GEO database with accession number GSE164298.

SUPPLEMENTAL MATERIAL

Supplemental material is available online only.

SUPPLEMENTAL FILE 1, PDF file, 1.7 MB.

ACKNOWLEDGMENTS

C.B., S.P., and J.M.L. performed all of the experiments with assistance from D.M.S.; C.B. and J.M.L. wrote the paper, with editorial assistance from all authors. J.M.L. conceived and supervised the study.

We thank Mark Zhang for his assistance in cloning plasmids used in this study.

This research was funded by an NSF grant to D.M.S. (1716794), an NIH grant to J.M.L. (AI090606), the Arnold and Mabel Beckman Foundation, the Camille and Henry Dreyfus Foundation, and Pomona College.

REFERENCES

1. Harris JB, LaRocque RC, Qadri F, Ryan ET, Calderwood SB. 2012. Cholera. *Lancet* 379:2466–2476. [https://doi.org/10.1016/S0140-6736\(12\)60436-X](https://doi.org/10.1016/S0140-6736(12)60436-X).
2. Kaper JB, Morris JG, Levine MM. 1995. Cholera. *Clin Microbiol Rev* 8:48–86. <https://doi.org/10.1128/CMR.8.1.48-86.1995>.
3. Deen J, Mengel MA, Clemens JD. 2020. Epidemiology of cholera. *Vaccine* 38:A31–A40. <https://doi.org/10.1016/j.vaccine.2019.07.078>.
4. Ali M, Nelson AR, Lopez AL, Sack DA. 2015. Updated global burden of cholera in endemic countries. *PLoS Negl Trop Dis* 9:e0003832. <https://doi.org/10.1371/journal.pntd.0003832>.
5. Silva AJ, Benítez JA. 2016. *Vibrio cholerae* biofilms and cholera pathogenesis. *PLoS Negl Trop Dis* 10:e0004330. <https://doi.org/10.1371/journal.pntd.0004330>.
6. Faruque SM, Nair GB. 2002. Molecular ecology of toxigenic *Vibrio cholerae*. *Microbiol Immunol* 46:59–66. <https://doi.org/10.1111/j.1348-0421.2002.tb02659.x>.
7. Houot L, Chang S, Absalon C, Watnick PI. 2010. *Vibrio cholerae* phosphoenolpyruvate phosphotransferase system control of carbohydrate transport, biofilm formation, and colonization of the germfree mouse intestine. *Infect Immun* 78:1482–1494. <https://doi.org/10.1128/IAI.01356-09>.
8. Galinier A, Deutscher J. 2017. Sophisticated regulation of transcriptional factors by the bacterial phosphoenolpyruvate: sugar phosphotransferase system. *J Mol Biol* 429:773–789. <https://doi.org/10.1016/j.jmb.2017.02.006>.
9. Deutscher J, Francke C, Postma PW. 2006. How phosphotransferase system-related protein phosphorylation regulates carbohydrate metabolism in bacteria. *Microbiol Mol Biol Rev* 70:939–1031. <https://doi.org/10.1128/MMBR.00024-06>.
10. Houot L, Chang S, Pickering BS, Absalon C, Watnick PI. 2010. The phosphoenolpyruvate phosphotransferase system regulates *Vibrio cholerae* biofilm formation through multiple independent pathways. *J Bacteriol* 192:3055–3067. <https://doi.org/10.1128/JB.00213-10>.
11. Hayes CA, Dalia TN, Dalia AB. 2017. Systematic genetic dissection of PTS in *Vibrio cholerae* uncovers a novel glucose transporter and a limited role for PTS during infection of a mammalian host. *Mol Microbiol* 104:568–579. <https://doi.org/10.1111/mmi.13646>.
12. Heidelberg JF, Eisen JA, Nelson WC, Clayton RA, Gwinn ML, Dodson RJ, Haft DH, Hickey EK, Peterson JD, Umayam L, Gill SR, Nelson KE, Read TD, Tettelin H, Richardson D, Ermolaeva MD, Vamathevan J, Bass S, Qin H, Dragoi I, Sellers P, McDonald L, Utterback T, Fleishmann RD, Nierman WC, White O, Salzberg SL, Smith HO, Colwell RR, Mekalanos JJ, Venter JC, Fraser CM. 2000. DNA sequence of both chromosomes of the cholera pathogen *Vibrio cholerae*. *Nature* 406:477–483. <https://doi.org/10.1038/35020000>.
13. Xu T, Cao H, Zhu W, Wang M, Du Y, Yin Z, Chen M, Liu Y, Yang B, Liu B. 2018. RNA-seq-based monitoring of gene expression changes of viable but non-culturable state of *Vibrio cholerae* induced by cold seawater. *Environ Microbiol Rep* 10:594–604. <https://doi.org/10.1111/1758-2229.12685>.
14. Mandlik A, Livny J, Robins WP, Ritchie JM, Mekalanos JJ, Waldor MK. 2011. RNA-Seq-based monitoring of infection-linked changes in *Vibrio cholerae* gene expression. *Cell Host Microbe* 10:165–174. <https://doi.org/10.1016/j.chom.2011.07.007>.
15. Frohman MA, Dush MK, Martin GR. 1988. Rapid production of full-length cDNAs from rare transcripts: amplification using a single gene-specific oligonucleotide primer. *Proc Natl Acad Sci U S A* 85:8998–9002. <https://doi.org/10.1073/pnas.85.23.8998>.
16. Papenfort K, Förstner KU, Cong J-P, Sharma CM, Bassler BL. 2015. Differential RNA-seq of *Vibrio cholerae* identifies the VqmR small RNA as a regulator of biofilm formation. *Proc Natl Acad Sci U S A* 112:E766–E775. <https://doi.org/10.1073/pnas.1500203112>.
17. Solovyev V, Salamov A. 2011. Automatic annotation of microbial genomes and metagenomic sequences, p 61–78. In Li RW (ed), *Metagenomics and its applications in agriculture, biomedicine, and environmental studies*. Nova Science Publishers, Hauppauge, NY.
18. Klucar L, Stano M, Hajduk M. 2010. phiSITE: database of gene regulation in bacteriophages. *Nucleic Acids Res* 38:D366–D370. <https://doi.org/10.1093/nar/gkp911>.
19. Deutscher J. 2008. The mechanisms of carbon catabolite repression in bacteria. *Curr Opin Microbiol* 11:87–93. <https://doi.org/10.1016/j.mib.2008.02.007>.
20. Ramseier TM, Bledig S, Michotey V, Feghali R, Saier MH. 1995. The global regulatory protein FruR modulates the direction of carbon flow in *Escherichia coli*. *Mol Microbiol* 16:1157–1169. <https://doi.org/10.1111/j.1365-2958.1995.tb02339.x>.
21. Ramseier TM, Nègre D, Cortay J-C, Scarabel M, Cozzzone AJ, Saier MH. 1993. *In vitro* binding of the pleiotropic transcriptional regulatory protein, FruR, to the *fru*, *pps*, *ace*, *pts* and *icd* operons of *Escherichia coli* and *Salmonella typhimurium*. *J Mol Biol* 234:28–44. <https://doi.org/10.1006/jmbi.1993.1561>.
22. Saier MH, Ramseier TM. 1996. The catabolite repressor/activator (Cra) protein of enteric bacteria. *J Bacteriol* 178:3411–3417. <https://doi.org/10.1128/jb.178.12.3411-3417.1996>.
23. Shimada T, Fujita N, Maeda M, Ishihama A. 2005. Systematic search for the Cra-binding promoters using genomic SELEX system. *Genes Cells* 10:907–918. <https://doi.org/10.1111/j.1365-2443.2005.00888.x>.
24. Yao R, Kurata H, Shimizu K. 2013. Effect of *cra* gene mutation on the metabolism of *Escherichia coli* for a mixture of multiple carbon sources. *ABB* 04:477–486. <https://doi.org/10.4236/abb.2013.43A063>.
25. Shimada T, Fujita N, Yamamoto K, Ishihama A. 2011. Novel roles of cAMP receptor protein (CRP) in regulation of transport and metabolism of carbon sources. *PLoS One* 6:e20081. <https://doi.org/10.1371/journal.pone.0020081>.
26. Feldheim DA, Chin AM, Nierva CT, Feucht BU, Cao YW, Xu YF, Sutrina SL, Saier MH. 1990. Physiological consequences of the complete loss of phosphoryl-transfer proteins HPr and FPr of the phosphoenolpyruvate:sugar phosphotransferase system and analysis of fructose (*fru*) operon expression in *Salmonella typhimurium*. *J Bacteriol* 172:5459–5469. <https://doi.org/10.1128/jb.172.9.5459-5469.1990>.
27. Chen B, Liang W, Wu R, Liang P, Kan B. 2013. Phenotype microarray screening of carbon sources used by *Vibrio cholerae* identifies genes regulated by the cAMP receptor protein. *Can J Microbiol* 59:472–478. <https://doi.org/10.1139/cjm-2013-0084>.
28. Fong JCN, Yıldız FH. 2008. Interplay between cyclic AMP-cyclic AMP receptor protein and cyclic di-GMP signaling in *Vibrio cholerae* biofilm formation. *J Bacteriol* 190:6646–6659. <https://doi.org/10.1128/JB.00466-08>.
29. Shimada T, Yamamoto K, Ishihama A. 2011. Novel members of the Cra regulon involved in carbon metabolism in *Escherichia coli*. *J Bacteriol* 193:649–659. <https://doi.org/10.1128/JB.01214-10>.
30. Browning DF, Busby SJW. 2004. The regulation of bacterial transcription initiation. *1. Nat Rev Microbiol* 2:57–65. <https://doi.org/10.1038/nrmicro787>.
31. Münch R, Hiller K, Grote A, Scheer M, Klein J, Schobert M, Jahn D. 2005. Virtual Footprint and PRODORIC: an integrative framework for regulon prediction in prokaryotes. *Bioinformatics* 21:4187–4189. <https://doi.org/10.1093/bioinformatics/bti635>.
32. Chavarria M, Fuhrer T, Sauer U, Pflüger-Grau K, de Lorenzo V. 2013. Cra regulates the cross-talk between the two branches of the phosphoenolpyruvate:

phosphotransferase system of *Pseudomonas putida*. Environ Microbiol 15:121–132. <https://doi.org/10.1111/j.1462-2920.2012.02808.x>.

33. Liu JM, Livny J, Lawrence MS, Kimball MD, Waldor MK, Camilli A. 2009. Experimental discovery of sRNAs in *Vibrio cholerae* by direct cloning, 5S/rRNA depletion and parallel sequencing. Nucleic Acids Res 37:e46. <https://doi.org/10.1093/nar/gkp080>.

34. Waters LS, Storz G. 2009. Regulatory RNAs in bacteria. Cell 136:615–628. <https://doi.org/10.1016/j.cell.2009.01.043>.

35. Carpousis AJ. 2007. The RNA degradosome of *Escherichia coli*: an mRNA-degrading machine assembled on RNase E. Annu Rev Microbiol 61:71–87. <https://doi.org/10.1146/annurev.micro.61.080706.093440>.

36. Mackie GA. 2013. RNase E: at the interface of bacterial RNA processing and decay. 1. Nat Rev Microbiol 11:45–57. <https://doi.org/10.1038/nrmicro2930>.

37. Davis BM, Waldor MK. 2007. RNase E-dependent processing stabilizes MicX, a *Vibrio cholerae* sRNA. Mol Microbiol 65:373–385. <https://doi.org/10.1111/j.1365-2958.2007.05796.x>.

38. Vercruyse M, Köhrer C, Davies BW, Arnold MFF, Mekalanos JJ, RajBhandary UL, Walker GC. 2014. The highly conserved bacterial RNase YbeY is essential in *Vibrio cholerae*, playing a critical role in virulence, stress regulation, and RNA processing. PLoS Pathog 10:e1004175. <https://doi.org/10.1371/journal.ppat.1004175>.

39. Yoon C-K, Kang D, Kim M-K, Seok Y-J. 2021. *Vibrio cholerae* FruR facilitates binding of RNA polymerase to the fru promoter in the presence of fructose 1-phosphate. Nucleic Acids Res 49:1397–1410. <https://doi.org/10.1093/nar/gkab013>.

40. Byer T, Wang J, Zhang MG, Vather N, Blachman A, Visser B, Liu JM. 2017. MtlR negatively regulates mannitol utilization by *Vibrio cholerae*. Microbiology (Reading) 163:1902–1911. <https://doi.org/10.1099/mic.0.000559>.

41. Folly BB, Ortega AD, Hubmann G, Bonsing-Vedelaar S, Wijma HJ, van der Meulen P, Milius-Argeitis A, Heinemann M. 2018. Assessment of the interaction between the flux-signaling metabolite fructose-1,6-bisphosphate and the bacterial transcription factors CggR and Cra. Mol Microbiol 109:278–290. <https://doi.org/10.1111/mmi.14008>.

42. Zhang MG, Liu JM. 2019. Transcription of cis antisense small RNA MtlS in *Vibrio cholerae* is regulated by transcription of its target gene, mtlA. J Bacteriol 201:e00178-19. <https://doi.org/10.1128/JB.00178-19>.

43. Li H. 2013. Aligning sequence reads, clone sequences and assembly contigs with BWA-MEM. ArXiv 1303.3997. <https://arxiv.org/abs/1303.3997>.

44. Anders S, Pyl PT, Huber W. 2015. HTSeq—a Python framework to work with high-throughput sequencing data. Bioinformatics 31:166–169. <https://doi.org/10.1093/bioinformatics/btu638>.

45. R Core Team. 2020. R: a language and environment for statistical computing. R Foundation for Statistical Computing, Vienna, Austria.

46. Love MI, Huber W, Anders S. 2014. Moderated estimation of fold change and dispersion for RNA-seq data with DESeq2. Genome Biol 15:550. <https://doi.org/10.1186/s13059-014-0550-8>.